

## Second-harmonic generation from chemically modified Ge(111) interfaces

Vasily Fomenko, Dora Bodlaki, Catherine Faler, and Eric Borguet<sup>a)</sup>

*Department of Chemistry and Surface Science Center, University of Pittsburgh, Pittsburgh, Pennsylvania 15260*

(Received 23 August 2001; accepted 3 January 2002)

Second-harmonic generation (SHG) was used to investigate chemically modified surfaces of Ge(111). Chemical modification was achieved by wet-chemical covalent binding of decyl and sulfur directly to the Ge interface after oxide stripping. Chemical modification of the interface substantially changes the second harmonic response. The decyl and sulfur terminations are stable in ambient during several weeks, as judged by SHG and XPS measurements. The SHG rotational anisotropy patterns were analyzed to estimate the relative values of the nonlinear susceptibilities describing the surface and bulk response. The choice of fundamental/SHG polarization combinations for accessing various nonlinear coefficients is presented. The factors affecting the relative values of the surface-to-bulk contributions to SHG and their changes upon chemical modification of the surface are discussed. In particular, it was found that the higher the electronegativity of chemically attached species, the higher the contribution of the surface-originating nonlinear terms to the overall response. Also, it was found that the relative contribution of surface versus bulk to SHG is different for different polarization combinations: the surface contribution to the *p*-in/*p*-out response is the greatest. © 2002 American Institute of Physics. [DOI: 10.1063/1.1454242]

### I. INTRODUCTION

The surface chemistry of semiconductors is of significant scientific and technological interest. The dominance of silicon, for example, in electronic devices is not so much as a consequence of its own properties, but rather those of its native oxide, SiO<sub>2</sub>.<sup>1,2</sup> SiO<sub>2</sub> is chemically stable with respect to materials used in microelectronics. As an excellent insulator possessing a sizeable bandgap (9 eV), SiO<sub>2</sub> provides a high barrier against injection of electrons from metals or silicon. It can be made relatively trap-free, so that carriers cannot be immobilized in it and degrade the device or its characteristics. SiO<sub>2</sub> forms a good barrier to diffusion at the high temperatures encountered in fabrication. Furthermore, the chemistry of SiO<sub>2</sub> is well known and understood.<sup>4</sup> SiO<sub>2</sub> can be etched in a controlled way and chemical groups attached to it with ease.

Silicon was not the first semiconductor material from which electronic devices were made. Indeed, the first semiconductor transistor was based on germanium.<sup>3</sup> The initial preference for germanium was due to its superior carrier transport properties—the mobilities of holes and electrons in Ge are more than twice those in Si.<sup>5</sup> Silicon, nevertheless, ultimately surpassed germanium because its oxide GeO<sub>2</sub>, which is water soluble, does not form a stable interface with the semiconductor and has higher trap/surface state density at its interface.<sup>6</sup> Surface chemistry, in particular a stable surface passivation, is key to the technological viability of Ge. Interest in Ge has renewed because of the ease with which it can be integrated with Si-based devices to fabricate emitters, modulators and receivers for optical communications, e.g.,

Ge-on-Si near-IR photodetectors. Semiconductor devices based on Si<sub>1-x</sub>Ge<sub>x</sub> alloys are already being commercialized.

Successful molecular electronics strategies seek to combine molecular chemistry with solid-state semiconductor technology via the chemical functionalization of semiconductor surfaces.<sup>7</sup> An important objective is to induce novel and useful chemical and physical properties while maintaining semiconductor interfaces that are electrically passive and stable under ambient conditions.<sup>7</sup> This explains the considerable interest in wet chemical modification of semiconductors that draws extensively on well-established, solution-phase organosilane and organogermanium chemistry, spurred on by the success in wet chemical H termination of Si.<sup>8,9</sup>

Many have studied both the effects of chemical modification of silicon surfaces with alkyl chains and various methods of achieving such monolayers. Several routes have been reported. Initially these involved radical chemistry or free radical initiation such as the notable work by Chidsey *et al.*<sup>10,11</sup> Photochemical routes to modification of silicon interfaces with terminal olefins were explored.<sup>12</sup> More recently, a halogenation/alkylation route with classic Grignard and organolithium reagents, as well as hydrosilation and direct reaction of alkyl magnesium bromide with Si-H, have been demonstrated.<sup>13,14</sup> Monolayers have also been prepared through Si-O-C covalent bonds and different terminal functional groups.<sup>15</sup> Functionalities, such as terminal esters, facilitate further chemical manipulation that can lead to new, e.g., biochemical, applications.<sup>16</sup>

Similar opportunities exist in Ge materials, though this is significantly less well established. Organic monolayers, e.g., alkyl chains, have been grafted to Ge(111) via a Grignard-type process.<sup>17</sup> Self-assembled monolayers of alkenes and alkynes have been grown on Ge(100) by Lewis-acid-mediated chemistry.<sup>18</sup>

<sup>a)</sup> Author to whom correspondence should be addressed. Electronic mail: borguet@pitt.edu

Various analytical techniques, including x-ray photoelectron spectroscopy (XPS), Fourier-transform infra-red spectroscopy (FTIR), Auger electron spectroscopy (AES), high-resolution energy loss spectroscopy (HREELS), contact angle measurements (CA), ellipsometry and second harmonic generation (SHG) have been employed to study chemically modified silicon surfaces.<sup>12–14,16,19–21</sup> The alkylated surfaces were found to be hydrophobic by contact angle measurements.<sup>19,22–24</sup> Ellipsometry has been used to determine the thickness of the overlayers.<sup>12,20,24</sup> XPS and FTIR were carried out to characterize the chemical composition of the interface and the degree of ordering of the organic monolayers.<sup>12,14,16,18–20</sup> SHG studies of chemically modified interfaces are of particular interest since they provide surface sensitivity and can be carried out *in situ*. SHG can probe buried interfaces that are difficult to probe by conventional spectroscopic methods.<sup>25</sup> The applicability of SHG to monitor charge, strain, microroughness as well as the progress of chemical reactions on semiconductor interfaces has been demonstrated.<sup>26–31</sup>

The present work investigates the changes of rotational anisotropy of SHG upon chemical modification of the surface as well as the mechanisms of such changes. We show that SHG can be used to probe the chemical state of the Ge interfaces. Special consideration is given to the procedure for estimating the relative surface and bulk contributions to SHG.

The article is organized as follows: Sec. II briefly describes the theory of SHG from semiconductor materials necessary for the analysis and interpretation of the data. Details of the procedure for separating the surface and bulk contributions to SHG are given. In Sec. III we describe the methods of sample preparation. In Sec. IV we describe the SHG experimental setup and characterization of the samples by ellipsometry and contact angle measurements. In Sec. V we present the experimental results and analysis with a particular emphasis given to the estimation of the relative magnitude of surface and bulk contributions to SHG. Possible microscopic mechanisms for the changes in SHG observed upon chemical termination of the surfaces are discussed.

## II. NONLINEAR OPTICAL PROBES OF SURFACES

Second harmonic generation from interfaces, the process of generation of light at the second-harmonic frequency of the incident fundamental radiation, is a sensitive probe of semiconductor interfacial structure.<sup>25</sup> Phenomenological theories of SHG were developed as early as the late 1960s for cubic and isotropic media.<sup>32–35</sup> These theories were developed for a thin ( $d \ll \lambda$ ) nonlinear slab at the interface between two linear media. These early SHG theories did not explicitly consider anisotropic SHG in accordance to the early SHG experimental data.<sup>32</sup> However, the subsequent observation of anisotropy in SHG from semiconductors<sup>36–40</sup> and metals<sup>41</sup> motivated a more detailed theoretical treatment of SHG from the interfaces of cubic materials.

Taking into account Fresnel coefficients for reflection and refraction, a phenomenological description of SHG from isotropic materials was achieved.<sup>42–44</sup> Subsequent studies provided a detailed description of SHG from crystals consid-

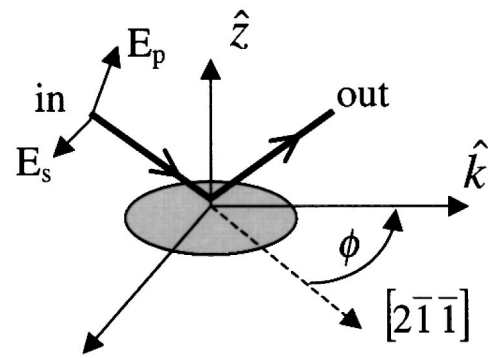


FIG. 1. Schematic of the rotational anisotropy experiment.  $\hat{k}$  is in the plane of incidence and parallel to the crystal surface.  $\hat{z}$  is in the plane of incidence and perpendicular to the crystal surface.  $\hat{s}$  is perpendicular to the plane of incidence and parallel to the crystal surface. The rotation of the crystal is tracked by the angle  $\phi$  between the  $[2\bar{1}\bar{1}]$  crystallographic direction and  $\hat{k}$ .

ering several sources of SHG signal: surface dipole, bulk quadrupole, and surface multipole terms arising from interfacial field gradients.<sup>45,46</sup> A way to estimate the relative magnitude of the bulk and the surface contributions was also described.<sup>38,45</sup> A number of excellent review articles describing second-order nonlinear optical probes of surfaces and interfaces are available.<sup>25,46–56</sup>

The result of the analysis by Sipe *et al.* can be summarized, for the (111) surface, as follows:

$$\frac{E_{p,p}(2\omega)}{E_p^2(\omega)} = [A_{pp} + B_{pp} \cos(3\phi)], \quad (1a)$$

$$\frac{E_{s,p}(2\omega)}{E_s^2(\omega)} = [A_{sp} + B_{sp} \cos(3\phi)], \quad (1b)$$

$$\frac{E_{p,s}(2\omega)}{E_p^2(\omega)} = B_{ps} \sin(3\phi), \quad (1c)$$

$$\frac{E_{s,s}(2\omega)}{E_p^2(\omega)} = B_{ss} \sin(3\phi), \quad (1d)$$

where  $\phi$  is the azimuthal angle measured between the plane of incidence and the  $[2\bar{1}\bar{1}]$  direction of the single crystal (Fig. 1).<sup>45,57</sup> The notation  $E_{s,p}(2\omega)$  denotes  $p$ -polarized SH generated by  $s$ -polarized fundamental. The constants  $A_{ij}$  and  $B_{ij}$  are specific to each of the four polarization combinations considered above and depend on the nonlinear coefficients, the angle of incidence and the linear Fresnel coefficients of the interface at the fundamental and second harmonic wavelengths:<sup>45</sup>

$$A_{pp} = A_p \left[ a_{1pp} \xi + a_{2pp} \left( \frac{\gamma}{\epsilon(2\omega)} + \partial_{31} \right) + a_{3pp} (\partial_{31} - \partial_{33}) + a_{4pp} \partial_{15} \right], \quad (2a)$$

$$B_{pp} = A_p [b_{1pp} \xi + b_{2pp} \partial_{11}], \quad (2b)$$

$$A_{sp} = A_p \left[ a_{1sp} \xi + a_{2sp} \left( \frac{\gamma}{\epsilon(2\omega)} + \partial_{31} \right) \right], \quad (2c)$$

$$B_{sp} = A_p [b_{1sp} \xi + b_{2sp} \partial_{11}], \quad (2d)$$

$$B_{ps} = A_s [b_{1ps} \xi + b_{2ps} \partial_{11}], \quad (2e)$$

$$B_{ss} = A_s [b_{1ss} \xi + b_{2ss} \partial_{11}]. \quad (2f)$$

The  $a$  and  $b$  coefficients as well as  $A_p$  and  $A_s$  in Eqs. (2) depend only on the linear dielectric parameters of the interface and the angle of incidence.<sup>45</sup> The nonlinear susceptibility coefficients  $\xi$ ,  $\gamma$  describe the bulk contributions and the  $\partial_{ij}$  describe that of the surface.

The constants  $A_{ij}$  and  $B_{ij}$  are, in general, complex. The following relationship exists between the complex-valued coefficients  $A_{pp}$  and  $B_{pp}$  having relative phase  $\theta_{pp}$ :

$$\frac{A_{pp}}{B_{pp}} = \frac{|A_{pp}|}{|B_{pp}|} \exp(i\theta_{pp}). \quad (3)$$

The  $p$ -in/ $p$ -out rotational anisotropy of SHG from the (111) face can be analyzed using the following equation:<sup>30</sup>

$$\begin{aligned} \frac{I_{pp}(2\omega)}{(I_p(\omega))^2} &\sim |A_{pp} + B_{pp} \cos(3\phi)|^2 \\ &= |A_{pp}|^2 + |B_{pp}|^2 \cos^2(3\phi) \\ &\quad + 2|A_{pp}|*|B_{pp}| \cos(3\phi) \cos(\theta_{pp}). \end{aligned} \quad (4)$$

A similar equation holds for the  $s$ -in/ $p$ -out polarization combination. The  $s$ -polarized SHG signal has only anisotropic contributions and is given by the following expressions:<sup>45</sup>

$$\frac{I_{ps}(2\omega)}{(I_p(\omega))^2} \sim |B_{ps} \sin(3\phi)|^2, \quad (5)$$

$$\frac{I_{ss}(2\omega)}{(I_s(\omega))^2} \sim |B_{ss} \sin(3\phi)|^2. \quad (6)$$

Equations (4)–(6) can be used to fit experimental SHG rotational anisotropy data to extract quantities proportional to the magnitudes of the  $A_{ij}$  and  $B_{ij}$  coefficients in Eqs. (1), as well as their relative phases. The  $A_{ij}$  and  $B_{ij}$  coefficients contain the complex-valued nonlinear coefficients;  $\xi$ ,  $\gamma$  and the  $\partial_{ij}$ .

The problem of separating bulk and surface contributions to SHG from cubic and isotropic media has been given attention in the literature. It should be noted that the  $A_{ij}$  and  $B_{ij}$  contain both surface and bulk terms. This is in large part the origin of the difficulty in separating surface and bulk contributions to SHG. It was reported that bulk and surface contributions to SHG are typically comparable and inseparable in a straightforward manner.<sup>58–60</sup> However, the relative magnitude of surface and bulk contributions depends essentially on the system. In the case of insulator surfaces, the surface and bulk contributions are likely to be comparable.<sup>59</sup> For metals and semiconductors, the ratio of surface-to-bulk contributions depends particularly on the state of the surface—for clean surfaces with highly polarizable surface bonds, e.g., Si(100)-(2×1), the surface contribution will dominate.<sup>58,59</sup>

The nonlinear coefficients ( $\partial_{33} - \partial_{31}$ ) and  $\partial_{15}$  are both present in the quantity  $A_{pp}$  [Eq. (2a)]. In order to access each of these coefficients independently, the SHG response pro-

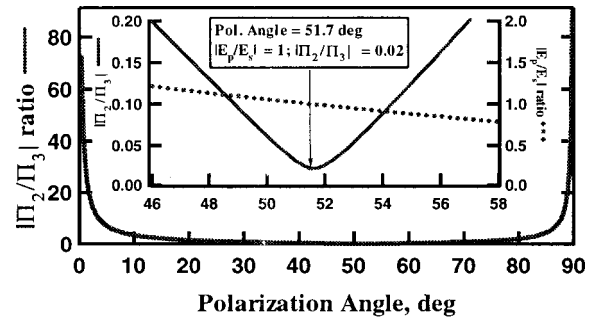


FIG. 2.  $|\Pi_2/\Pi_3|$  of Eq. (8) (solid line) and ratio of  $p$ - and  $s$ -field amplitudes (dotted line) as functions of the polarization angle at Ge interface at  $\lambda_\omega = 800$  nm, at  $45^\circ$  angle of incidence. The field amplitudes are evaluated inside the material.

duced by mixed excitation, with both  $s$ -in and  $p$ -in present, should be analyzed.<sup>30,61,62</sup> In the case of  $s$ -polarized output, we can obtain

$$\begin{aligned} E_s^{2\omega}(111) &= A_s \left[ \left( \frac{4}{3} \Gamma \xi f_c + 2\partial_{15} i \tilde{\Omega} \right) E_s E_p f_s + \right. \\ &\quad + A_s \left[ \frac{2\sqrt{2}}{3} f_c (f_c^2 E_p^2 - E_s^2 - 2f_s^2 E_p^2) \xi \Gamma \right. \\ &\quad \left. \left. + \partial_{11} (f_c^2 E_p^2 - E_s^2) i \tilde{\Omega} \right] \sin(3\phi) \right. \\ &\quad \left. + A_s \left[ \left\{ -\frac{4\sqrt{2}}{3} (f_c^2 - f_s^2) \xi \Gamma \right. \right. \right. \\ &\quad \left. \left. \left. - 2\partial_{11} f_c i \tilde{\Omega} \right\} E_s E_p \right] \cos(3\phi), \end{aligned} \quad (7)$$

where the complex-valued coefficients  $f_s = \sin \theta/n$  and  $f_c = \sqrt{1 - f_s^2}$  describe the propagation of the fundamental in the medium,  $\theta$  is the angle of incidence and  $n$  is the ratio, at the fundamental frequency, of the complex-valued refractive indices of the media that constitute the interface.<sup>45</sup>  $\Gamma$  and  $\tilde{\Omega}$  are complex-valued functions, containing the propagation vectors and the wavelength of the fundamental at the interface.<sup>45</sup> The fundamental field amplitudes are evaluated inside the material.

Equation (7) contains an isotropic term, with no dependence on  $\phi$ , and two anisotropic terms containing  $\sin(3\phi)$  and  $\cos(3\phi)$ . Equation (7) can be rewritten in a more compact form as

$$I_{\text{mix-in/s-out}}^{2\omega} = |\Pi_1 + \Pi_2 \sin(3\phi) + \Pi_3 \cos(3\phi)|^2 I^2(\omega). \quad (8)$$

The analysis of mixed-in,  $s$ -out polarization in the form of Eq. (8) is complicated, involving five fitting parameters: three moduli of  $\Pi_1$ ,  $\Pi_2$ ,  $\Pi_3$  and two phase differences between any two given pairs of the  $\Pi_i$  coefficients. Equation (8) can, in principle, be simplified by a suitable choice of the relative magnitudes of  $E_s$  and  $E_p$ , i.e., the polarization angle, to eliminate  $\Pi_2$  or  $\Pi_3$ . The ratio  $|\Pi_2/\Pi_3|$ , as a function of the polarization angle for Ge at 800 nm, is shown in Fig. 2.  $|\Pi_2/\Pi_3|$  approaches zero at the polarization angle of

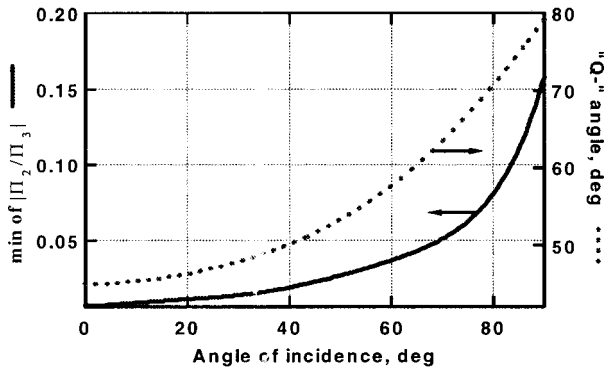


FIG. 3. Optimization of mixed-in/s-out polarization combination at  $\lambda_\omega = 800$  nm on Ge. The minimum value of  $|\Pi_2/\Pi_3|$  [Eq. (8)] as a function of the angle of incidence (solid line). The polarization angle,  $Q$ -angle, to minimize  $|\Pi_2/\Pi_3|$  of Eq. (8) as a function of the angle of incidence (dashed line).

$51.7^\circ$  (Fig. 2), close to the value of  $50.0^\circ$  found for Si near 800 nm.<sup>30</sup> At this angle, the  $\Pi_2$  term becomes negligible and Eq. (8) can be approximated as

$$I_{q\text{-in}/s\text{-out}}^2 = |\Pi_1 + \Pi_3 \cos(3\phi)|^2 I^2(\omega). \quad (9)$$

We denote the mixed-in/s-out polarization that minimizes  $\Pi_2$  as  $q$ -in/s-out following the notation of Mitchell *et al.*<sup>30</sup> Having just two complex-valued parameters simplifies the analysis because it requires only three fitting parameters. The polarization angle at which the  $|\Pi_2/\Pi_3|$  ratio is minimized corresponds to equal  $p$ - and  $s$ -polarized field amplitudes inside the medium, i.e.,  $|E_p/E_s|=1$  in Fig. 2. This finding is consistent with that of Mitchell *et al.* where SHG response of  $q$ -in/s-out polarization was described by Eq. (9) rather than Eq. (8).<sup>30</sup> However, it should be noted that Eq. (9) is an approximation. At the polarization angle, selected as described above, the ratio  $|\Pi_2/\Pi_3|$  does not go to zero (Fig. 2). While the approximation may be valid here, there are cases when neglecting the  $\Pi_2$  term in Eq. (8) may not be a good approximation. For example, the ratio  $|\Pi_2/\Pi_3|$  increases to 0.15 at grazing incidence. The variation of  $|\Pi_2/\Pi_3|$ , as well as the polarization angle minimizing  $|\Pi_2/\Pi_3|$ , as a function of the angle of incidence at 800 nm for Ge are shown in Fig. 3.

Why isn't there a polarization angle at which the term  $\Pi_2$  vanishes? It is clear, from Eq. (7), that the surface contribution to the  $\Pi_2$  term cancels out when  $E_s = f_c E_p$ . This corresponds to the case when the horizontal components of  $s$ - and  $p$ -polarized fundamental fields inside the material are equal.<sup>61,62</sup> However, the bulk contribution, i.e., the term with  $\xi$ , remains. In order for  $\Pi_2$  to vanish, the system of equations

$$\begin{aligned} f_c^2 E_p^2 - E_s^2 - 2 f_s^2 E_p^2 &= 0, \\ f_c^2 E_p^2 - E_s^2 &= 0 \end{aligned} \quad (10)$$

should be satisfied. This is possible only at normal angle of incidence ( $f_s = 0$ ). Therefore, some contribution to the  $\Pi_2$  term in Eq. (8), from either surface or from the bulk, will always be present at non-normal incidence.

The choice of polarization angle to simplify Eq. (8) by minimizing the  $\Pi_2$  term requires separate consideration and

*a priori* knowledge of the  $|\partial_{11}|/|\xi|$  ratio and its phase,  $\Delta(\partial_{11}/\xi)$ . These quantities can be estimated by the method first suggested by Tom *et al.*<sup>38</sup> This method involves comparing the relative ratio of  $s$ -polarized SHG signals from the (111) and (100) surfaces. By doing so, one obtains a relative measurement of the following quantities,

$$|B_{ps}^{(100)}| = |a_{ps}^{(100)} \xi|, \quad (11)$$

$$|B_{ps}^{(111)}| = |b_{1ps} \xi + b_{2ps} \partial_{11}|, \quad (12)$$

where  $a_{ps}^{(100)}$ ,  $b_{1ps}$ ,  $b_{2ps}$  are known functions.<sup>45</sup> Comparing the SHG efficiencies for  $p$ -in/s-out SHG from Ge(111) and Ge(100) gives the ratio of  $|B_{ps}^{(111)}|/|B_{ps}^{(100)}|$  and, in turn, yields a range of possible  $|\partial_{11}|/|\xi|$  ratios and corresponding relative phases. These quantities can also be obtained from  $s$ -in/s-out measurements but this signal is usually lower in amplitude and, therefore, is subject to greater error. However, it does provide a check of consistency without providing a basis for selecting the relative phase of the  $|\partial_{11}|/|\xi|$  quantities. Although this method is quite straightforward, it is sensitive to the possible differences in surface preparation and structure that might affect the magnitude of the fields inside the material.<sup>45</sup>

Obtaining the relative phases of  $\xi$  and  $\partial_{11}$  together with the ratio of their magnitudes, by comparing SHG signals from two different samples, requires special experimental efforts, e.g., performing phase-sensitive SHG measurements from each sample.<sup>46,63,64</sup> From measurements of SHG intensity alone, we can obtain only a range for the ratio  $|\partial_{11}|/|\xi|$ , for all the possible phase differences between  $\xi$  and  $\partial_{11}$ . Nevertheless, this method has been applied, giving insight into the behavior of the nonlinear susceptibilities as well as providing a starting point to the estimation of the other nonlinear susceptibilities.<sup>30,38,45,65</sup>

The following sequence of steps can be suggested to evaluate the relative values of surface versus bulk nonlinear coefficients:

- (1) Compare the  $p$ -in/s-out SHG from the (111) and (100) surfaces to obtain  $|\partial_{11}|/|\xi|$  and their relative phases. The  $s$ -in/s-out measurements can be used to check the consistency of the results.
- (2) Use the results of step 1 to analyze the  $s$ -in/ $p$ -out SHG output to extract  $|\gamma/\varepsilon(2\omega) + \partial_{31}|/|\xi|$  and their relative phase. Here, some assumption of the phase between  $|\partial_{11}|$  and  $|\xi|$  is needed. Following the literature, we used the value of  $\pi$  for the phase difference.<sup>30,66</sup> It is to be noted that, for a phase difference of  $\pi$ , the ratio  $|\partial_{11}|/|\xi|$  reaches its maximum. In principle, similar analysis done for the (100) surface can be used as a consistency check since the  $s$ -in/ $p$ -out SHG at the (100) surface is described by the same combination of nonlinear coefficients.
- (3) Use the results of step 1 and the SHG rotational anisotropy for  $q$ -in/s-out SHG to estimate the  $|\partial_{15}|/|\xi|$  and its relative phase.
- (4) Use the results of steps 1–3 to analyze the  $p$ -in/ $p$ -out SHG to estimate  $|\partial_{33} - \partial_{31}|/|\xi|$  and its phase.
- (5) As a final step, the values obtained for the nonlinear coefficients and their relative phases, in steps 1–4, were used as parameters for Eqs. (1) to estimate the  $A_{ij}$ ,  $B_{ij}$

and  $\theta_{ij}$  rotational anisotropy coefficients, and compared with the experimentally determined SHG rotational anisotropy coefficients.

It is to be noted, however, that only limited separation of the bulk and surface susceptibilities is possible. For example, the separation of  $\gamma/\varepsilon(2\omega)$  and  $\partial_{31}$ , as well as accessing  $\partial_{33}$  and  $\partial_{31}$  individually is not possible. One can only estimate the combinations of  $(\gamma/\varepsilon(2\omega) + \partial_{31})$  and  $(\partial_{33} - \partial_{31})$  relative to  $\xi$ .

This procedure was applied to oxidized and chemically modified Ge surfaces to estimate the influence of the chemical modification on the relative values of the nonlinear coefficients. An important approximation was made: any differences in the linear dielectric constants of the oxide-covered and chemically modified Ge were neglected. Moreover, since the oxide and chemical overlayers were thin, the dielectric functions of the media on the Ge interfaces were taken to be those of vacuum. This is equivalent to neglecting the small effect of a thin dielectric layer on the linear optical properties of the system. In addition, any contributions to SHG arising from gradients of nonlinear susceptibilities at interfaces were neglected.<sup>59</sup>

### III. PREPARATION OF SAMPLES

Ge wafers (undoped, Eagle Picher) were degreased by successive 10 min sonications in trichloroethylene (J. T. Baker, reagent grade), acetone (EM Science, reagent grade), then methanol (Fisher Scientific, certified ACS grade). No additional treatment was performed on oxidized samples before experiments. All chemicals were purchased from Aldrich Co., unless otherwise stated, and used as received. For chemical modification, the clean, oxidized Ge samples were first hydrogen terminated by dipping in 48% HF (Mallinckrodt, reagent grade) five times for 10 s, each time followed by a 20 s rinse in nanopure water.<sup>67</sup> Alkylated Ge was prepared by the halogenation/alkylation procedure employed for Si(111).<sup>13</sup> After hydrogen termination, the Ge sample was exposed to a solution of  $\text{PCl}_5$  in deoxygenated chlorobenzene using benzoyl peroxide as a radical initiator, in a flask under Ar (99.99%), and gently warmed for 30 min. Following removal of the chlorobenzene solution, the sample was rinsed with fresh, deoxygenated chlorobenzene, while still in the flask and under Ar. Once the chlorobenzene was completely removed, decylmagnesium bromide (1M in ether) was introduced into the flask and allowed to react at room temperature for 24 h. After the reaction was complete, the sample was rinsed with anhydrous ether to remove unreacted reagent. Once taken out of the flask, the Ge sample was sonicated for 10 min each in methanol then dichloromethane. Sulfidation of the Ge(111) surface was achieved by immersion of H-terminated Ge in  $(\text{NH}_4)_2\text{S}$  at 70 °C for 20 min, then rinsing in MeOH and drying by  $\text{N}_2$  flow.<sup>68,69</sup>

The chemically modified samples were found to be stable in air for at least several weeks as judged by the reproducibility of the SHG rotational anisotropy measurements and by the absence of the characteristic oxide peak in XPS measurements performed on samples exposed to ambient for 4 weeks.

### IV. EXPERIMENT

The second harmonic generation experiments were performed with a sub-100-fs Ti:sapphire oscillator (Coherent Mira Seed), pumped by all lines of an  $\text{Ar}^+$  laser (Coherent Innova 310), operating at a repetition rate of 76 MHz. Equipped with a birefringent filter and a set of custom optics, the oscillator was tunable from 720 to 930 nm. Light incident at 45° angle with respect to the surface normal was focused with a 100 mm lens. The spot diameter was determined by the knife-edge technique ( $1/e^2$  criterion) to be  $32 \pm 2 \mu\text{m}$  yielding a peak power density of  $1.8 \times 10^9 \text{ W/cm}^2$  at  $\lambda = 800 \text{ nm}$  for a 70 fs pulse. The bandwidth of the fundamental was 8 nm at 800 nm and that of SHG was 4 nm. Rotation of the sample about its normal axis (azimuthal rotation) was under computer control. Care was taken to minimize the intensity variations of the reflected light produced by the wobble of the sample when rotated about its normal axis. The power of the incident beam was controlled by a waveplate/polarizer combination and held at 111 mW ( $\sim 1.5 \text{ nJ/pulse}$ ,  $1.3 \times 10^{-4} \text{ J/cm}^2$ ) throughout the experiments. This fluence is below the damage threshold and no indications of irreversible damage were detected during the experiments. The literature reports the damage threshold to be on the order of  $\sim 0.1 \text{ J/cm}^2$  of pulsed irradiation in picosecond and femtosecond range in wavelength range of 700–800 nm for Si and Ge.<sup>40,70</sup> The quadratic behavior of SHG was verified in the power range explored.<sup>71</sup> Reflected second harmonic signals were detected by single photon counting after spectral filtering with a filter/monochromator/red-blind PMT combination. Polarizers with extinction coefficients better than  $5 \times 10^{-5}$  determined the polarization of the incident fundamental and the reflected second harmonic light. Care was taken to detect pure *s*- or *p*-polarization as the reflected second harmonic light typically contained two to three orders of magnitude more *p*- than *s*-polarized light depending on the azimuth.

Water contact angles were measured with a VCA-2000 contact angle apparatus. The advancing contact angles ( $\Theta_a$ ) from a drop of water delivered by a 22 gauge flat stainless steel needle were measured immediately after deposition. At least four measurements were made, providing typical error of  $\pm 2^\circ$ . Well-ordered alkane layers on Si with high coverage will approach advancing angles of  $100^\circ$ .<sup>11,20,21,24,72</sup> Contact angles as large as  $109^\circ$  for reactions of silicon with dodecene, dodecanol, and hexadecene have been reported.<sup>19,21,23</sup> Dodecyl contact angles as high as  $112^\circ$  were reported for a thermal reaction of Si with 1-dodecene.<sup>11</sup> These angles provide a suitable comparison for the decyl monolayers used in this study. Ge(111)-(CH<sub>2</sub>)<sub>9</sub>CH<sub>3</sub> samples prepared with this procedure had contact angles as high as  $99 \pm 2^\circ$ , which compares favorably with the literature for alkyl-Ge:  $\Theta_a = 95^\circ$ .<sup>18</sup> Compared to the contact angles on oxidized Ge,  $\Theta_a$  on degreased Ge/GeO<sub>2</sub> was  $50^\circ$ , the significant increase of the contact angle indicates the formation of hydrophobic organic layers. Contact angles on alkyl-Ge surfaces are consistently lower than those on alkyl-Si.<sup>18</sup> The use of organometallics (EtAlCl<sub>2</sub>-initiated, Grignard) for Si alkylation is reported to yield lower contact angles as compared to thermal or UV-initiated routes.<sup>18</sup> The

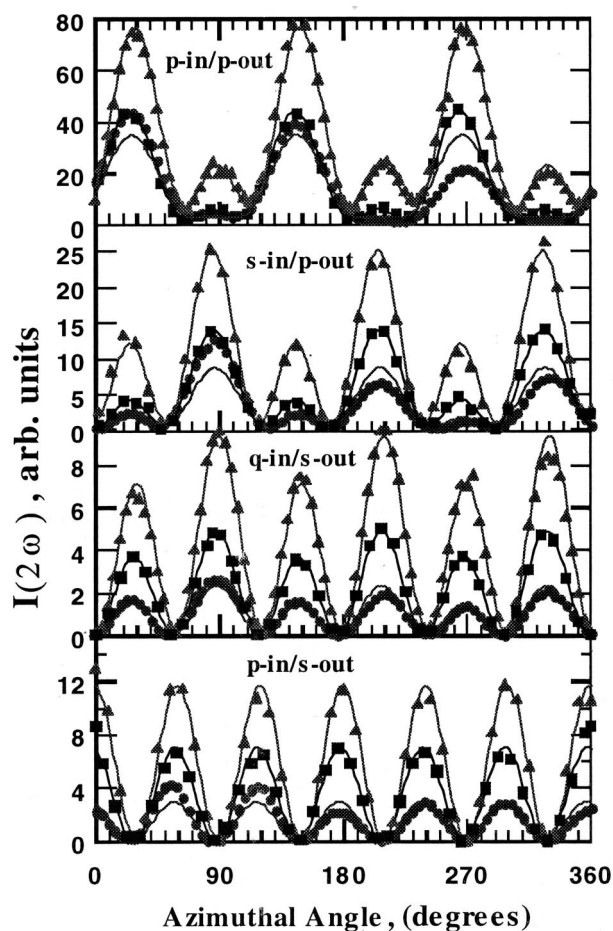


FIG. 4. Second harmonic generation rotational anisotropy for chemically modified Ge(111) surfaces at  $\lambda_{\omega} = 800$  nm, at  $45^{\circ}$  angle of incidence. N.B. In this figure, the azimuthal angle,  $\phi$ , is that between the plane of incidence and the  $[01\bar{1}]$  vector on the (111) plane.  $\blacktriangle$  Ge-oxide,  $\blacksquare$  Ge-alkyl, and  $\bullet$  Ge-S.

contact angle on the Ge(111)-S surface was measured to be  $(70 \pm 2)^{\circ}$ .

## V. ROTATIONAL ANISOTROPY OF CHEMICALLY MODIFIED Ge(111) SURFACES AT 800 nm. RESULTS AND DISCUSSION

### A. Qualitative description of data and comparison to Si

The SHG rotational anisotropy for natively oxidized, decyl-terminated and sulfur-terminated Ge(111) samples in air at 800 nm fundamental wavelength are shown in Fig. 4 for various polarization combinations. The data reflect the changes in SHG rotational anisotropy induced by chemical modification. The *p*-in/*p*-out, *s*-in/*p*-out and *q*-in/*s*-out rotational anisotropy patterns show a threefold symmetry with three small and three large peaks separated by  $120^{\circ}$  with a weak isotropic offset above the background. Obvious is the decrease of the magnitude of the small peaks in *p*-in/*p*-out, *s*-in/*p*-out and *q*-in/*s*-out polarization combinations as well as the overall decrease of the signal as the surface termination is changed from oxide to alkyl to sulfide. The observed changes can be used as a basis for separating the contributions of the

TABLE I. SHG rotational anisotropy coefficients ( $A_{ij}$ ,  $B_{ij}$  and  $\theta_{ij}$ ) of chemically modified Ge(111) relative to  $|A_{pp}|$  of the oxidized surface at  $\lambda_{\omega} = 800$  nm, at  $45^{\circ}$  angle of incidence. N.B. ( $B_{p\text{-in/s-out}}^{(111)}/B_{p\text{-in/s-out}}^{(100)}$ )<sub>oxide</sub> =  $15.8 \pm 0.4$ .

Coefficient	Ge(111) surface		
	Ge-Oxide	Ge-Alkyl	Ge-S
$ A_{pp} $	1.00	0.82	0.86
$ B_{pp} $	1.80	1.20	0.93
$\theta_{pp}$	51	35	34
$ A_{sp} $	0.39	0.35	0.31
$ B_{sp} $	1.20	0.81	0.59
$\theta_{sp}$	127	136	142
$ A_{qs} $	0.15	0.10	0.11
$ B_{qs} $	0.83	0.60	0.39
$\theta_{qs} $	113	117	115
$ B_{ps} $	1.00	0.78	0.51

surface and the bulk to the SHG response. Chemical termination should change mainly the surface properties while leaving the bulk intact.

The qualitative trends in the observed changes in the rotational anisotropy of chemically modified Ge have both similarities and differences to those reported for chemically modified Si(111) at 830 nm.<sup>30</sup> A trend that is common for both Si(111) and Ge(111) is the overall decrease of the SHG signal with the surface modification from oxide to alkyl.<sup>30</sup> However, for the Si(111) surface, the decylation led to an increase of the relative ratio of the small/large peaks, while in the case of Ge at 800 nm the small peaks decreased relative to the large ones. The small peaks were also observed to decrease relative to the large peaks upon chemical modification of Ge(111) at 824 nm. Therefore, the origin of difference with Si is material dependent, not wavelength dependent.

The rotational anisotropy data were fit with Eqs. (4)–(6) and Eq. (9). Table I represents the magnitudes of isotropic  $A_{ij}$  and anisotropic  $B_{ij}$  coefficients, referenced to the  $A_{pp}$  coefficient, derived from the analysis. The trends in the behavior of the  $A_{ij}$  and  $B_{ij}$  coefficients for various Ge(111) surfaces are represented in Fig. 5. Also shown in Fig. 5, by the horizontal lines, is the contribution of the bulk anisotropic response,  $\xi$ , at 800 nm.

Table II lists the values of the extracted nonlinear susceptibilities relative to the bulk anisotropic susceptibility,  $\xi$ . As noted above, the bulk anisotropic response,  $\xi$ , contributes to all the isotropic,  $A_{ij}$ , and anisotropic,  $B_{ij}$ , coefficients of Eqs. (2). To evaluate the contribution of  $\xi$  to the  $A_{ij}$  and  $B_{ij}$ , the magnitude of  $\xi$  was evaluated from the *p*-in/*s*-out SHG on (100), i.e., the quantity  $B_{ps}^{(100)}$  of Eq. (11). Then, the evaluated value of  $\xi$  was substituted in Eqs. (2) describing the  $A_{ij}$  and  $B_{ij}$  with all the other susceptibilities  $\gamma$  and  $\partial_{ij}$  set equal to zero to determine the contribution of  $\xi$ . It is interesting to note that for some cases, the contribution of the bulk anisotropic susceptibility,  $\xi$ , alone is greater than the contribution of the coefficients, e.g.,  $B_{ps}$  and  $B_{qs}$  that contain both  $\xi$  and  $\partial_{11}$ . This is simply a consequence of the phase difference of  $\pi$  between the bulk  $\xi$  and surface  $\partial_{11}$  contributions, i.e., destructive interference between these coherent SHG source terms.

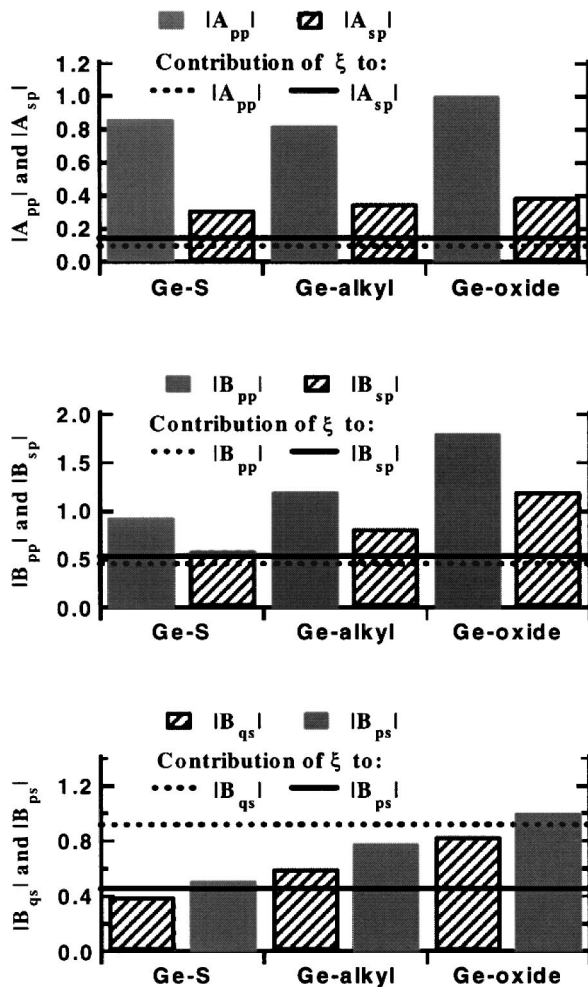


FIG. 5. SHG rotational anisotropy coefficients ( $A_{ij}$  and  $B_{ij}$ ) for chemically modified Ge(111) surfaces referenced to  $|A_{pp}|$  of the oxidized surface. The horizontal lines show the contribution of the bulk anisotropic response,  $\xi$ , to the  $A_{ij}$  and  $B_{ij}$  at  $\lambda_\omega=800$  nm and  $45^\circ$  angle of incidence.

**B. Trends in the  $A_{ij}$ ,  $B_{ij}$  and the nonlinear susceptibility coefficients. Comparison to chemically modified Si**

The graphs in Fig. 5 as well as the data in Table II show certain trends in the behavior of the nonlinear susceptibilities for the chemically modified Ge(111) surfaces. First of all, it is seen that, in general, the efficiency of SHG, as judged from the  $A_{ij}$  and  $B_{ij}$  coefficients, is greater for oxidized surfaces than for the alkyl- or S-terminated surfaces. One can also see that the relative contribution of the anisotropic bulk susceptibility,  $\xi$ , to the SHG response, represented by the horizontal lines in Fig. 5, increases from oxidized to alky-

lated to S-terminated surface. Supposing that the remaining contribution comes from the surface-related terms,  $\partial_{ij}$ , one can suggest that the removal of the oxide and termination of the surface by alkyl or sulfur quenches the magnitude of the surface response. The phase changes caused by alkylation and sulfidation are minor, as seen from Table II. Second, in Fig. 5, one can see that the contribution of the bulk anisotropic susceptibility,  $\xi$ , to the  $A_{pp}$  components is relatively small for all surface terminations but its contribution to all the other components ( $A_{sp}, B_{pp}, B_{sp}, B_{ps}$ ) is considerable. Also, as one can observe from Table II, the ratio of the surface-to-bulk nonlinear susceptibilities decreases from the oxidized to the alkylated to the S-terminated surface.

As mentioned in the Introduction, the calculations of the nonlinear susceptibilities were performed neglecting the dielectric functions of the overlayers. This approximation seems to be valid because the overlayers were thin, much thinner than the wavelength of the fundamental light. However, in order to justify the validity of such an approximation a check-up calculation of the quantity  $|\partial_{11}/\xi|$  was performed considering the chemically modified Ge interface to lie between bulk Ge and bulk alkane, rather than between bulk Ge and vacuum. However, the analysis does not change the general trend in the behavior of the  $|\partial_{11}/\xi|$  value—the decrease of  $|\partial_{11}/\xi|$  from oxidized to alkylated to S-terminated surface is still present. Moreover, the magnitude of  $|\partial_{11}/\xi|$  changes at most by 50%.

**C. Chemical origin of the trends in the nonlinear optical coefficients**

The observed trends can be understood by considering the Ge(111) interface as a network of terminated surface bonds, polarized according to the nature of the chemical bonding at the interface.<sup>30,56</sup> The surface bonds, as well as the Ge–Ge backbonds, may be polarized due to chemical bonding at the interface. The polarization of the surface bonds should increase the SHG response as noticed in SHG experiments on Si(100) with variable H-coverage in UHV—saturation of silicon dangling bond with hydrogen quenched the SHG response.<sup>73</sup> In addition, strain at the interface due to lattice mismatch between the oxide and the substrate can affect the SHG.<sup>74</sup> The trends in the nonlinear susceptibility coefficients, presented in Table II, suggest that influence of the electronegativity of the surface bonds may be more significant than the influence of the lattice mismatch. The electronegativity of oxygen is greater than that of carbon and sulfur (3.44 for O, 2.55 for C and 2.58 for S, 2.01 for Ge).<sup>75</sup>

TABLE II. Nonlinear susceptibility coefficients and their phases for chemically modified Ge in air at  $\lambda_\omega=800$  nm.

Ge(111) surface	$ \partial_{11} / \xi $	$\Delta(\partial_{11}/\xi)$	$ \gamma/\epsilon + \partial_{31} / \xi $	$\Delta((\gamma/\epsilon + \partial_{31})/\xi)$	$ \partial_{15} / \xi $	$\Delta(\partial_{15}/\xi)$	$ \partial_{33} - \partial_{31} / \xi $	$\Delta((\partial_{33} - \partial_{31})/\xi)$
Ge-Oxide	0.205	$1.00\pi$	0.0156	$1.71\pi$	0.200	$0.625\pi$	1.93	$0.445\pi$
Ge-Alkyl	0.169	$1.00\pi$	0.0144	$1.74\pi$	0.155	$0.670\pi$	1.49	$0.496\pi$
Ge-S	0.144	$1.00\pi$	0.0129	$1.75\pi$	0.170	$0.635\pi$	1.43	$0.369\pi$

The electronegativity difference provides a measure of the polarity of a bond between two atoms. Consequently, with the Ge–O bonds being most polar, the rotational anisotropy patterns change the most from the oxidized to the alkylated to the sulfidated surface. The change in going from the alkylated to the sulfidated surface is less than from the oxidized to the alkylated surface. These results suggest that the electronegativity perturbation of the surface bonds is an important factor changing the SHG response. Similar observations were made for the Si(111) and Si(100) interfaces.<sup>30,73,76,77</sup> Changes in SHG response were associated with the change in the polarization of surface bonds rather than surface strain.<sup>30,73,76,77</sup> Moreover, deposition of 1–2 ML of Ge on the surface of Si(100) was found to increase the SHG signal but this effect was reversed again by H-termination.<sup>76</sup> The H-termination was reported to preserve interfacial lattice mismatch strain caused by Ge deposition and therefore, structural, strain-based mechanisms were found to be inconsistent with the observed trends.<sup>56</sup>

It is also worth noting that the polarization of both Ge–Ge backbones and chemical-terminated Ge surface bonds is important in determining the surface-derived SHG response. The results in Table II show that all the  $|\partial_{ij}|/|\xi|$  values change with chemical termination. The  $\partial_{ij}$  coefficients describe the purely local, surface dipole contribution to SHG. If the surface response were changing solely due to the polarization of the dangling bonds, only the coefficients involving  $\partial_{33}$  would be expected to change, since the susceptibility  $\partial_{33}$  describes the SHG solely due to polarization changes perpendicular to the interface.<sup>30</sup> The polarization of surface backbonds, oriented at non-normal angles to the interface, can be expected to be sensed by  $\partial_{ij}$  coefficients other than  $\partial_{33}$ .

From inspection of the data in Table II, an observation can be made about the relative contribution of surface and bulk to SHG. The ratio of the surface-derived coefficients  $\partial_{ij}$  to the bulk-derived coefficient  $\xi$  is less than 1 for all cases except  $|(\partial_{33} - \partial_{31})/|\xi|$ . Furthermore, the contribution of the  $\xi$  component is small only in the case of the  $A_{pp}$  coefficient. This observation suggests that only in the case of the *p*-in/*p*-out combination, that alone contains the  $\partial_{33}$  component, is the SHG response localized strongly near the surface. For all the other polarization combinations the contribution of the bulk cannot be neglected. The strong surface contribution to the *p*-in/*p*-out SHG as opposed to *s*-in/*p*-out and *q*-in/*s*-out SHG, for which bulk contributions supply most of the intensity, was observed in UHV experiments on Si(100) reconstructed by H, B or Ge.<sup>56,73,76,77</sup> The interpretation of strong surface localization of the *p*-in/*p*-out SHG and significant bulk contribution to *s*-in/*p*-out and *q*-in/*s*-out SHG was supported by calculations of SHG driven solely by surface terms.<sup>56</sup> It was found that the SHG intensity should be approximately three orders of magnitude weaker in *s*-in/*p*-out and *q*-in/*s*-out combinations than in *p*-in/*p*-out, while the experimentally observed signals were only about one order of magnitude weaker.<sup>56</sup> The difference in the localization of SHG at the surface of Si and Ge can be the reason for the difference in the changes in SHG caused by chemical modification of these two materials. The recent study by Mitchell

*et al.* shows that in the case of Si(111), the contribution of the bulk,  $\xi$ , even to the *p*-in/*p*-out SHG, is larger than that of the surface terms; the ratio of surface-to-bulk nonlinear susceptibilities is less than 1 in all cases (Table 3 in Ref. 30).<sup>30</sup> In the case of Ge, as can be seen from the quantity  $|\partial_{33} - \partial_{31}|/|\xi|$  in Table II, the SHG signal is more strongly surface localized for *p*-polarized SHG output. This stronger surface localization of SHG in the case of Ge is in part a consequence of the linear optical properties of the material. The penetration depth, estimated from the extinction coefficient as  $l = \lambda/4\pi k$ , of the fundamental in Ge,  $\sim 80$  nm, is over an order of magnitude smaller than in Si,  $\sim 1720$  nm. Therefore, the fundamental polarizes a thinner layer of bulk in Ge. More importantly, the penetration depth of UV light, i.e., the depth from which second harmonic can radiate to the ambient, is also smaller for Ge: 15 nm for Ge versus 79 nm for Si at 400 nm. Therefore, the relative contributions of surface and bulk to SHG are determined in part by the penetration depths of fundamental and second harmonic wavelengths.

Some comments should be presented on the procedure of extracting the relative values of the  $\partial_{ij}$ . The determination of the nonlinear susceptibility coefficients and their phases is ambiguous since, at each step of the procedure, there is an ambiguity regarding the sign of the relative phases of the parameters  $\theta_{sp}$ ,  $\theta_{qs}$  and  $\theta_{pp}$ . This ambiguity arises from the fact that the experimental fitting procedure, involving  $\cos(\theta_{pp})$ ,  $\cos(\theta_{sp})$ , and  $\cos(\theta_{qs})$  cannot yield the sign of the phase difference. Both positive and negative phase differences satisfy Eqs. (4) and (9). However, all the possible outcomes may be examined and the trends arising from chemical modification can be explored.

Let us now address this ambiguity of the determination of the magnitude of the nonlinear susceptibilities and their phases, arising from the negative or positive choice of phase difference in  $A_{ij}$  and  $B_{ij}$  coefficients. Depending on the positive or negative choice of the phase between  $A_{qs}$  and  $B_{qs}$ , the magnitude of  $|\partial_{15}/\xi|$  does not change significantly, while its phase does change considerably—by as much as  $\pi$ . Both the magnitude and the phase of  $|\gamma/\epsilon_2 + \partial_{31}|/|\xi|$  are affected by the choice of a positive or negative phase difference between  $A_{pp}$  and  $B_{pp}$ . The value  $|\partial_{33} - \partial_{31}|/|\xi|$  and its phase are the most poorly determined because the ambiguities in the phases,  $\theta_{sp}$ ,  $\theta_{qs}$ ,  $\Delta(\partial_{15}/|\xi|)$ ,  $\Delta(|\gamma/\epsilon_2 + \partial_{31}|/|\xi|)$  and  $\theta_{pp}$  are accumulated as well as the error in determining the magnitudes of  $|\gamma/\epsilon_2 + \partial_{31}|/|\xi|$ ,  $|\partial_{15}/|\xi|$  and  $|\partial_{11}|/|\xi|$ . Nevertheless, all the possible outcomes may be examined and generalizations can be made about the behavior of the nonlinear susceptibilities.

For the  $|\partial_{33} - \partial_{31}|/|\xi|$ , eight combinations of the signs of the relative phases, corresponding to positive/negative phases  $\theta_{sp}$ ,  $\theta_{qs}$  and  $\theta_{pp}$  can be explored. Table III lists the results for all the eight possibilities for Ge/GeO<sub>2</sub>. The general trends in the nonlinear susceptibilities from oxidized to alkylated to S-terminated remain the same for all the possible combinations of the relative phases. In particular, the surface-to-bulk ratio,  $|\partial_{33} - \partial_{31}|/|\xi|$ , decreases in going from oxide to alkyl to S. The surface-to-bulk nonlinear susceptibility ratio of alkyl- and S-terminated surfaces is similar, consistent with the similarity in electronegativity of C and S.



TABLE III. The effect of the choice of the signs of  $\theta_{pp}$ ,  $\theta_{sp}$ ,  $\theta_{qs}$  on the nonlinear susceptibility coefficients of the Ge/GeO<sub>2</sub> interface at  $\lambda_\omega = 800$  nm.<sup>a</sup>

Combination no.	1	2	3	4	5	6	7	8
$ \partial_{11} / \xi $					0.21			
$\Delta(\partial_{11}/\xi)$					$1.00\pi$			
$\theta_{qs}$		113		-113		113		-113
$\theta_{sp}$		127		127		-127		-127
$\theta_{pp}$	51	-51	51	-51	51	-51	51	-51
$ \partial_{15} / \xi $		0.200		0.230		0.200		0.230
$\Delta(\partial_{15}/\xi)$		$0.625\pi$		$1.260\pi$		$0.625\pi$		$1.260\pi$
$ \gamma/\varepsilon + \partial_{31} / \xi $		0.0156		0.0156		0.0085		0.0085
$\Delta((\gamma/\varepsilon + \partial_{31})/\xi)$		$1.71\pi$		$1.71\pi$		$0.487\pi$		$0.487\pi$
$\Delta((\partial_{33} - \partial_{31})/\xi)$	$0.445\pi$	$1.88\pi$	$0.441\pi$	$1.84\pi$	$0.290\pi$	$1.630\pi$	$0.250\pi$	$1.63\pi$
$ \partial_{33} - \partial_{31} / \xi $	1.93	0.600	1.83	0.673	0.759	1.68	0.705	1.78
$ B_{pp}/A_{pp} $	1.80	1.80	1.82	1.80	1.80	1.81	1.79	1.81
$ B_{pp}/A_{pp} $				1.8				
Experimental <sup>b</sup>								
$\theta_{pp}$ , (degrees)	51.0	-51.0	51.9	-50.9	50.9	-52.0	50.9	-50.6
$ \theta_{pp} $ (degrees)				51				
Experimental <sup>b</sup>								

<sup>a</sup>The 8 possible combinations of the relative phases— $\theta_{pp}$ ,  $\theta_{sp}$ ,  $\theta_{qs}$ —of the experimental SHG rotational anisotropy coefficients result in different values of the nonlinear susceptibilities while yielding values of the rotational anisotropy coefficients consistent with experiment.

<sup>b</sup>See Table I.

The nonlinear susceptibilities in Table II are those for positive relative phases of the  $A_{ij}$  and  $B_{ij}$  rotational anisotropy coefficients. The value of  $|\partial_{33} - \partial_{31}|/|\xi|$  is consistently larger for Ge than for Si surfaces. To check the validity of the analysis, all the possible values of the nonlinear susceptibilities along with the possible phases were used to calculate the rotational anisotropy patterns. The resultant rotational anisotropy patterns reproduced the experimental data, and were practically indistinguishable irrespective of the choice of combinations of signs of the relative phases. The calculated patterns therefore do not provide a means for resolving the sign ambiguity, but do provide a check of consistency of the analysis.

## VI. CONCLUSIONS

SHG from surfaces of Ge(111), modified by wet chemical treatments, was investigated. Contributions to SHG from bulk and surface terms were determined and compared. Contributions from bulk and surface are comparable for most polarization combinations. The  $p$ -in/ $p$ -out combination, however, seems to be dominated by the surface response. The effects of chemical modification on SHG are discussed in terms of changes of polarization of the surface bonds and surface backbonds, as well as effects associated with surface strain. The surface contribution to SHG diminishes when less electronegative species are bound to the surface, a consequence of reducing the polarization of the surface bonds. The phenomenological dependence of  $s$ -polarized second harmonic generated by mixed-polarized input is analyzed as a function of the angle of incidence and the polarization angle. The optimal choice of the polarization angle to simplify the analysis and corresponding approximations are presented.

## ACKNOWLEDGMENTS

The authors acknowledge the support of the National Science Foundation, CHE-9734273. The courtesy of Profes-

sor Chapman for the use of the ellipsometer and contact angle apparatus for sample characterization is appreciated. The assistance of Mr. Hiromichi Yamamoto and Professor D. Waldeck with XPS measurements is acknowledged. The authors thank Professor M. C. Downer for making available a preprint of his recent review article. Helpful discussions with Dr. S. Mitchell are appreciated.

<sup>1</sup>A. B. Fowler, Phys. Today **October**, 59 (1993).

<sup>2</sup>A. B. Fowler, Phys. Today **October**, 50 (1997).

<sup>3</sup>J. Bardeen and W. H. Brattain, Phys. Rev. **74**, 230 (1948).

<sup>4</sup>Y. J. Chabal, *Fundamental Aspects of Silicon Oxidation* (Springer, Berlin, 2001).

<sup>5</sup>C. Kittel, *Introduction to Solid State Physics*, 6th ed. (Wiley, New York, 1986).

<sup>6</sup>P. Balk, in *The Si-SiO<sub>2</sub> System*, edited by P. Balk (Elsevier, Amsterdam, 1988), Vol. 32, pp. 2–20.

<sup>7</sup>R. A. Wolkow, Annu. Rev. Phys. Chem. **50**, 413 (1999).

<sup>8</sup>J. M. Buriak, Chem. Commun. (Cambridge) **12**, 1051 (1999).

<sup>9</sup>G. J. Pietsch, Appl. Phys. A: Mater. Sci. Process. **60**, 347 (1995).

<sup>10</sup>M. R. Linford and C. E. D. Chidsey, J. Am. Chem. Soc. **115**, 12631 (1993).

<sup>11</sup>M. R. Linford, P. Fenter, P. M. Eisenberger, and C. E. D. Chidsey, J. Am. Chem. Soc. **117**, 3145 (1995).

<sup>12</sup>R. L. Cicero, M. R. Linford, and C. E. D. Chidsey, Langmuir **16**, 5688 (2000).

<sup>13</sup>A. Bansal, X. L. Li, I. Lauermann, N. S. Lewis, S. I. Yi, and W. H. Weinberg, J. Am. Chem. Soc. **118**, 7225 (1996).

<sup>14</sup>R. Boukherroub, S. Morin, F. Bensebaa, and D. D. M. Wayner, Langmuir **15**, 3831 (1999).

<sup>15</sup>R. Boukherroub, S. Morin, P. Sharpe, D. D. M. Wayner, and P. Allongue, Langmuir **16**, 7429 (2000).

<sup>16</sup>R. Boukherroub and D. D. M. Wayner, J. Am. Chem. Soc. **121**, 11513 (1999).

<sup>17</sup>J. L. He, Z. H. Lu, S. A. Mitchell, and D. D. M. Wayner, J. Am. Chem. Soc. **120**, 2660 (1998).

<sup>18</sup>K. Choi and J. M. Buriak, Langmuir **16**, 7737 (2000).

<sup>19</sup>A. B. Sieval, A. L. Demirel, J. W. M. Nissink, M. R. Linford, J. H. van der Maas, W. H. de Jeu, H. Zuilhof, and E. J. R. Sudholter, Langmuir **14**, 1759 (1998).

<sup>20</sup>P. Wagner, S. Nock, J. A. Spudich, W. D. Volkmuth, S. Chu, R. L. Cicero, C. P. Wade, M. R. Linford, and C. E. D. Chidsey, J. Struct. Biol. **119**, 189 (1997).

- <sup>21</sup>X. Y. Zhu, V. Boiadjev, J. A. Mulder, R. P. Hsung, and R. C. Major, *Langmuir* **16**, 6766 (2000).
- <sup>22</sup>F. Effenberger, G. Gotz, B. Bidlingmaier, and M. Wezstein, *Angew. Chem. Int. Ed. Engl.* **37**, 2462 (1998).
- <sup>23</sup>A. B. Sieval, V. Vleeming, H. Zuilhof, and E. J. R. Sudholter, *Langmuir* **15**, 8288 (1999).
- <sup>24</sup>A. Y. Fadeev and T. J. McCarthy, *Langmuir* **16**, 7268 (2000).
- <sup>25</sup>G. Lüpke, *Surf. Sci. Rep.* **35**, 75 (1999).
- <sup>26</sup>J. I. Dadap, P. T. Wilson, M. H. Anderson, and M. C. Downer, *Opt. Lett.* **22**, 901 (1997).
- <sup>27</sup>J. Fang and G. P. Li, *Appl. Phys. Lett.* **75**, 3506 (1999).
- <sup>28</sup>W. Daum, H. J. Krause, U. Reichel, and H. Ibach, *Phys. Rev. Lett.* **71**, 1234 (1993).
- <sup>29</sup>J. I. Dadap, B. Doris, Q. Deng, M. C. Downer, J. K. Lowell, and A. C. Diebold, *Appl. Phys. Lett.* **64**, 2139 (1994).
- <sup>30</sup>S. A. Mitchell, R. Boukherroub, and S. Anderson, *J. Phys. Chem. B* **104**, 7668 (2000).
- <sup>31</sup>S. A. Mitchell, M. Mehendale, D. M. Villeneuve, and R. Boukherroub, *Surf. Sci.* **488**, 367 (2001).
- <sup>32</sup>N. Bloembergen, R. K. Chang, S. S. Jha, and C. H. Lee, *Phys. Rev.* **174**, 813 (1968); *Phys. Rev. Lett.* **178**, 1528 (E) (1969).
- <sup>33</sup>N. Bloembergen and P. S. Pershan, *Phys. Rev.* **128**, 606 (1962).
- <sup>34</sup>C. C. Wang and W. W. Duminski, *Phys. Rev. Lett.* **20**, 668 (1968).
- <sup>35</sup>C. C. Wang, *Phys. Rev.* **178**, 1457 (1969).
- <sup>36</sup>T. A. Driscoll and D. Guidotti, *Phys. Rev. B* **28**, 1171 (1983).
- <sup>37</sup>D. Guidotti, T. A. Driscoll, and H. J. Gerritsen, *Solid State Commun.* **46**, 337 (1983).
- <sup>38</sup>H. W. K. Tom, T. F. Heinz, and Y. R. Shen, *Phys. Rev. Lett.* **51**, 1983 (1983).
- <sup>39</sup>J. A. Litwin, H. M. van Driel, and J. E. Sipe, *Mater. Res. Soc. Symp. Proc.* **35**, 125 (1985).
- <sup>40</sup>J. A. Litwin, J. E. Sipe, and H. M. Van Driel, *Phys. Rev. B* **31**, 5543 (1985).
- <sup>41</sup>H. W. K. Tom and G. D. Aumiller, *Phys. Rev. B* **33**, 8818 (1986).
- <sup>42</sup>P. Guyot-Sionnest, W. Chen, and Y. R. Shen, *Phys. Rev. B* **33**, 8254 (1986).
- <sup>43</sup>J. E. Sipe, *J. Opt. Soc. Am. B* **4**, 481 (1987).
- <sup>44</sup>V. Mizrahi and J. E. Sipe, *J. Opt. Soc. Am. B* **5**, 660 (1988).
- <sup>45</sup>J. E. Sipe, D. L. Moss, and H. M. van Driel, *Phys. Rev. B* **35**, 1129 (1987).
- <sup>46</sup>T. F. Heinz, in *Nonlinear Surface Electromagnetic Phenomena*, edited by H.-E. Ponath and G. I. Stegeman (Elsevier, Amsterdam, 1991), pp. 353–416.
- <sup>47</sup>Y. R. Shen, *Nature (London)* **337**, 519 (1989).
- <sup>48</sup>Y. R. Shen, *Annu. Rev. Phys. Chem.* **40**, 327 (1989).
- <sup>49</sup>G. L. Richmond and R. A. Bradley, in *Laser Spectroscopy and Photochemistry on Metal Surface*, edited by H. L. Dai and W. Ho (Elsevier, New York, 1992), Vol. I, pp. 132–183.
- <sup>50</sup>H. M. van Driel, *Appl. Phys. A: Mater. Sci. Process.* **59**, 545 (1994).
- <sup>51</sup>*Second-Order Nonlinear Optical Effects at Surfaces and Interfaces: Recent Advances*, edited by G. F. Reider and T. F. Heinz (Elsevier, Amsterdam, 1995).
- <sup>52</sup>J. F. McGilp, *J. Phys. D* **29**, 1812 (1996).
- <sup>53</sup>J. F. McGilp, *Surf. Rev. Lett.* **6**, 529 (1999).
- <sup>54</sup>N. Bloembergen, *Appl. Phys. B: Lasers Opt.* **68**, 289 (1999).
- <sup>55</sup>Y. R. Shen, *IEEE J. Sel. Top. Quantum Electron.* **6**, 1375 (2000).
- <sup>56</sup>M. C. Downer, B. S. Mendoza, and V. I. Gavrilenko, *Surf. Interface Anal.* **31**, 966 (2001).
- <sup>57</sup>O. A. Aktsipetrov, A. A. Fedyanin, V. N. Golovkina, and T. V. Murzina, *Opt. Lett.* **19**, 1450 (1994).
- <sup>58</sup>P. Guyot-Sionnest and Y. R. Shen, *Phys. Rev. B* **35**, 4420 (1987).
- <sup>59</sup>P. Guyot-Sionnest and Y. R. Shen, *Phys. Rev. B* **38**, 7985 (1988).
- <sup>60</sup>X. D. Zhu and A. Wong, *Phys. Rev. B* **46**, 2540 (1992).
- <sup>61</sup>H. W. K. Tom, Ph.D. thesis, University of California, 1984.
- <sup>62</sup>R. W. J. Hollering, *J. Opt. Soc. Am. B* **8**, 374 (1991).
- <sup>63</sup>B. Pettinger and C. Bilger, *Chem. Phys. Lett.* **286**, 355 (1998).
- <sup>64</sup>C. Bilger and B. Pettinger, *Chem. Phys. Lett.* **294**, 425 (1998).
- <sup>65</sup>O. A. Aktsipetrov, I. M. Baranova, and Y. A. Il'inskii, *Sov. Phys. JETP* **64**, 167 (1986).
- <sup>66</sup>G. Lüpke, D. J. Bottomley, and H. M. van Driel, *J. Opt. Soc. Am. B* **11**, 33 (1994).
- <sup>67</sup>T. Deegan and G. Hughes, *Appl. Surf. Sci.* **123**, 66 (1998).
- <sup>68</sup>G. W. Anderson, M. C. Hanf, P. R. Norton, Z. H. Lu, and M. J. Graham, *Appl. Phys. Lett.* **66**, 1123 (1995).
- <sup>69</sup>P. F. Lyman, O. Sakata, D. L. Marasco, T. L. Lee, K. D. Breneman, D. T. Keane, and M. J. Bedzyk, *Surf. Sci.* **462**, L594 (2000).
- <sup>70</sup>J. I. Dadap, X. F. Hu, N. M. Russell, J. G. Ekerdt, J. K. Lowell, and M. C. Downer, *IEEE J. Sel. Top. Quantum Electron.* **1**, 1145 (1995).
- <sup>71</sup>V. Fomenko, J. F. Lami, and E. Borguet, *Phys. Rev. B* **63**, 121316 (2001).
- <sup>72</sup>A. B. Sieval, R. Opitz, H. P. A. Maas, M. G. Schoeman, G. Meijer, F. J. Vergeldt, H. Zuilhof, and E. J. R. Sudholter, *Langmuir* **16**, 10359 (2000).
- <sup>73</sup>J. I. Dadap, Z. Xu, X. F. Hu, M. C. Downer, N. M. Russell, J. G. Ekerdt, and O. A. Aktsipetrov, *Phys. Rev. B* **56**, 13367 (1997).
- <sup>74</sup>G. Erley, R. Butz, and W. Daum, *Phys. Rev. B* **59**, 2915 (1999).
- <sup>75</sup>See *CRC Handbook* (CRC, Boca Raton, 1998), pp. 9–74.
- <sup>76</sup>P. S. Parkinson, D. Lim, R. Büngener, J. G. Ekerdt, and M. C. Downer, *Appl. Phys. B* **68**, 641 (1999).
- <sup>77</sup>D. Lim, M. C. Downer, J. G. Ekerdt, N. Arzate, B. S. Mendoza, V. I. Gavrilenko, and R. Q. Wu, *Phys. Rev. Lett.* **84**, 3406 (2000).